

Highly Nonlinear Solitary Waves in Periodic Dimer Granular Chains

Mason A. Porter¹, Chiara Daraio^{2*}, Eric B. Herbold³, Ivan Szelenowicz⁴, and P. G. Kevrekidis⁵

¹*Department of Physics and Center for the Physics of Information,*

²*Graduate Aeronautical Laboratories (GALCIT) and Department of Applied Physics,
California Institute of Technology, Pasadena, CA 91125, USA*

³*Department of Mechanical and Aerospace Engineering,*

University of California at San Diego, La Jolla, California 92093-0411, USA

⁴*Département de Mécanique, Ecole Polytechnique, 91128 Palaiseau cedex, France*

⁵*Department of Mathematics and Statistics, University of Massachusetts, Amherst MA 01003-4515, USA*

We report the propagation of highly nonlinear solitary waves in heterogeneous, periodic granular media using experiments, numerical simulations, and theoretical analysis. We examine periodic arrangements of particles in experiments in which stiffer/heavier beads (stainless steel) are alternated with softer/lighter ones (PTFE beads). We find excellent agreement between experiments and numerics in a model with Hertzian interactions between adjacent beads, which in turn agrees very well with a theoretical analysis of the model in the long-wavelength regime that we derive for heterogeneous environments and general bead interactions. Our analysis encompasses previously-studied examples as special cases and also provides key insights on the influence of the dimer lattice on the properties (width and propagation speed) of the obtained highly nonlinear wave solutions.

PACS numbers: 05.45.Yv, 43.25.+y, 45.70.-n, 46.40.Cd

Over the past several years, the highly nonlinear dynamic response of granular materials has drawn increased attention from the scientific community [1, 2, 3, 4, 5, 6, 7, 8, 9, 10, 11, 12, 13, 14, 15, 16]. The corresponding theory developed for uniform lattice systems [1] supports the formation of a novel type of wave in materials, setting a paradigm for the design and creation of systems with unprecedented properties. A simple setup for the study of highly nonlinear dynamics in solids is provided by one-dimensional (1D) granular media consisting of chains of interacting spherical particles that deform elastically when they collide. The broad interest in such systems has arisen because they possess qualitatively different features from weakly nonlinear systems. For example, their solitary-wave solutions have a finite support that is independent of their amplitude [1], providing perhaps the most experimentally tractable application of the notion of “compactons” [17]. There have also been a number of recent studies on the effects of defects (i.e., inhomogeneities, particles with different masses, etc.) in such systems, allowing the observation of interesting physical responses such as fragmentation, anomalous reflections, and energy trapping [4, 5, 6, 8, 9, 10, 11, 12, 15]. Moreover, chains of granular media have been shown to be highly tunable [1, 2, 3] and have the potential to be used in many engineering applications – including shock and energy absorbing layers [9, 10, 11, 12], sound focusing devices (tunable acoustic lenses and delay lines), sound absorption layers, and sound scramblers [13, 14].

A class of phenomena for which 1D chains of granular media provide an ideal setting concerns the interplay between nonlinearity and periodicity. The study of nonlinear oscillator chains has a time-honored history, originating with the Fermi-Pasta-Ulam problem [18, 19, 20]. Its applications arise in numerous areas of physics, includ-

ing coupled waveguide arrays and photorefractive crystals in nonlinear optics [21, 22], Bose-Einstein condensates in optical lattices in atomic physics [23], and DNA double-strand dynamics in biophysics [24]. A particular theme that often arises in this context is that of “heterogeneous” versus “uniform” lattices. Here, we focus on the prototypical heterogeneity of “dimers” (i.e., chains of beads made of alternating materials). This topic is of interest to a diverse array of physical settings ranging from ferroelectric perovskites [25, 26] and polymers [27] to optical waveguides [28] and cantilever arrays [29]. Chains of beads provide a particularly interesting and versatile setting with which to study such problems because of their strong nonlinearity and the wide range of available material properties (and concomitant tunability) [2, 3, 10, 13, 14].

Our aim in the present work is to investigate solitary wave propagation in chains of granular dimers [30] combining experiments, numerical simulations, and theoretical analysis. Some preliminary results on dimer chains are discussed in [1]. In this Letter, we consider a broad class of configurations consisting of stainless steel:PTFE (polytetrafluoroethylene) [13, 14] dimer chains with different periodicities (obtained by varying the number of consecutive steel particles). We report very good agreement between experiments and numerics. We also apply a long-wavelength approximation to the nonlinear lattice model to obtain a quasi-continuum nonlinear partial differential equation (PDE) description of the system. Because of the chain lengths and the pulse amplitudes considered in our experimental and numerical analyses, the pulse propagation can be safely assumed to be within the highly nonlinear regime and the effects of gravity in the theoretical analysis have been neglected, in accordance with the discussion of [7]. We obtain analytical expres-

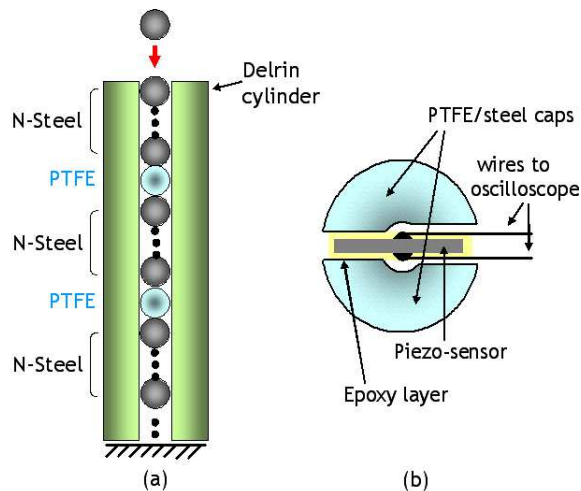


FIG. 1: (Color online) (a) Experimental setup for dimer chain consisting of a periodic array of N consecutive stainless steel beads interspersed with 1 PTFE bead. (b) Schematic diagram of the composition of the sensors placed in the chain.

sions for wave solutions of the PDE and find very good agreement between the widths and propagation speeds of these solutions with those obtained from experiments and numerical simulations.

Experimental Setup. The experimental dimer chains were composed of vertically aligned beads in a delrin guide that contained slots for sensor connections. Each “ $N : 1$ dimer” (see Fig. 1) included a variable number $N \in \{1, \dots, 7\}$ of the high-modulus, large mass stainless steel beads (non-magnetic, 316 type) alternating with a single low-modulus, small mass PTFE bead in a periodic sequence. The diameter of all spheres was 4.76 mm, and the number of beads in the chain was 38. Three piezo-sensors were embedded inside the particles in the system, as described in [10, 13, 14]. The calibrated sensors ($RC \approx 10^3 \mu s$) were connected to a four-channel Tektronix Oscilloscope (TKTDS 2014), allowing direct visualization of the propagating pulse via force versus time curves and time-of-flight calculations of the pulse speed. Waves were generated by a striker (a 0.45 g stainless steel bead) dropped from various heights. The steel beads had mass 0.45 g, elastic modulus 193 GPa, and Poisson ratio 0.3 [31, 32]; and the PTFE beads had mass 0.123 g, elastic modulus 1.46 GPa, and Poisson ratio 0.46 [13, 33]. Previous studies of dimer chains only considered materials with similar elastic moduli [1].

Numerical simulations. We model a chain of n spherical beads as a 1D lattice with Hertzian interactions be-

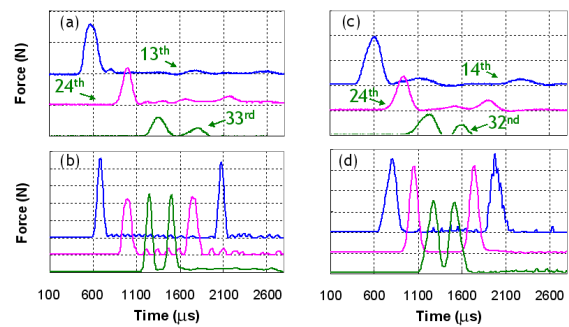


FIG. 2: (Color online) Force versus time response obtained from chains of dimers consisting of (a,b) 1 or (c,d) 2 stainless steel beads alternating with 1 PTFE bead. Panels (a,c) show experimental results, and (b,d) show the corresponding numerical data. The striker has a velocity of 1.37 m/s on impact and the y -axis scale is 2 N per division. The numbered arrows point to the corresponding particles in the chain. In both configurations, the second curve (showing the results for particle 24) represents a PTFE bead and the other curves represent steel beads.

tween beads [1]:

$$\ddot{y}_j = \frac{A_{j-1,j}}{m_j} \delta_j^{3/2} - \frac{A_{j,j+1}}{m_j} \delta_{j+1}^{3/2} + g, \quad (1)$$

$$A_{j,j+1} = \frac{4E_j E_{j+1} \left(\frac{R_j R_{j+1}}{R_j + R_{j+1}} \right)^{1/2}}{3 [E_{j+1} (1 - \nu_j^2) + E_j (1 - \nu_{j+1}^2)]},$$

where y_j is the coordinate of the center of the j th particle, $j \in \{1, \dots, n\}$, $\delta_j \equiv \max\{y_{j-1} - y_j, 0\}$ for $j \in \{2, \dots, n\}$, $\delta_1 \equiv 0$, $\delta_{n+1} \equiv \max\{y_n, 0\}$, g is the gravitational acceleration, E_j is the Young’s modulus of the j th bead, ν_j is its Poisson ratio, m_j is its mass, and R_j is its radius. The particle $j = 1$ represents the steel striker, and the $(n + 1)$ st particle represents the wall (i.e., an infinite-radius particle that cannot be displaced). The initial velocity of the striker is determined by experiments and all other particles start at rest in their equilibrium positions.

In Fig. 2, we show the very good agreement between experimental and numerical results for 1 : 1 [panels (a,b)] and 2 : 1 [panels (c,d)] dimers of steel:PTFE particles. For the 1 : 1 dimers, the dynamics indicate that the initial excited impulse develops into a solitary wave within the first 10 particles of the chain. We also obtain robust pulses for $N : 1$ dimers with $N > 1$ (with N as high as 7 in experiments and as high as 22 in numerics), though the transient dynamics and spatial widths of the developed solitary-like waves are different.

Theoretical Analysis. We focus our analysis on the prototypical 1 : 1 dimer chain with beads of different masses (denoted m_1 and m_2). The rescaled equations of motion (without gravity; see the discussion below) can

be written [1]

$$m_1 \ddot{u}_j = (w_j - u_j)^k - (u_j - w_{j-1})^k, \quad (2)$$

$$m_2 \ddot{w}_j = (u_{j+1} - w_j)^k - (w_j - u_j)^k, \quad (3)$$

where u_j (w_j) denotes the displacement of the j th sphere of mass m_1 (m_2). We consider a general power-law interaction to illustrate the comprehensiveness of our approach and use Hertzian contact ($k = 3/2$) to compare our theoretical analysis with our numerical and experimental results.

The distance from u_j to w_j (from u_j to u_{j+1}) is D ($2D$). Using D as a small parameter, we develop a long-wavelength approximation (LWA) by Taylor-expanding Eqs. (2)-(3), for which we express u_{j+1} (w_{j-1}) as a function of u_j (w_j). The resulting PDEs need to be ‘‘homogenized’’ between the two ‘‘species’’. To accomplish this, we follow [34], postulating a ‘‘consistency condition’’ between the two fields:

$$w = \lambda (u + b_1 D u_x + b_2 D^2 u_{xx} + b_3 D^3 u_{xxx} + b_4 D^4 u_{4x} + \dots). \quad (4)$$

We then self-consistently determine the coefficients λ and b_i by demanding that Eqs. (2) and (3) are identical at *each order*. (Note that the subscripts in the LWA denote derivatives.) The parameter λ can take the values 1 (for acoustic excitations) or $-m_1/m_2$ (for optical ones). The nature of our experimental initial conditions *generically* leads to in-phase waveforms, so we restrict our considerations to $\lambda = 1$ hereafter [35]. Considering the ensuing PDE at orders D^k - D^{k+3} , we find that $b_1 = 1$, $b_2 = m_1/(m_1 + m_2)$, $b_3 = (2m_1 - m_2)/[3(m_1 + m_2)]$, and $b_4 = m_1(m_1^2 - m_1 m_2 + m_2^2)/[3(m_1 + m_2)^3]$. Observe that these results correctly capture the uniform-chain limit of $m_1 = m_2$, for which w should represent the Taylor expansion of radius D around u .

The resulting PDE,

$$u_{\tau\tau} = u_x^{k-1} u_{xx} + G u_x^{k-3} u_{xx}^3 + H u_x^{k-2} u_{xx} u_{xxx} + I u_x^{k-1} u_{4x}, \quad (5)$$

has the same form (with different coefficients) as that obtained for uniform chains [1]. In Eq. (5), $\tau = 2D^{k+1}tk/(m_1 + m_2)$ is a rescaled time, $G = D^2(2 - 3k + k^2)m_1^2/[6(m_1 + m_2)^2]$, $H = 2D^2(k - 1)(2m_1^2 + m_1 m_2 - m_2^2)/[6(m_1 + m_2)^2]$, and $I = 2D^2(m_1^2 - m_1 m_2 + m_2^2)/[6(m_1 + m_2)^2]$. We seek traveling-wave solutions $u \equiv u(\xi)$, with $\xi = x - V_s t$, and obtain an ordinary differential equation (ODE) for $u_\xi = v$. We then change variables with the transformation $v = z^p$, where the power p is chosen so that terms proportional to $z^{p-3}z_\xi^3$ disappear in the resulting ODE for $z = z(\xi)$. Finally, an integrating factor z^a , with $a = 1 - kp + 3(p - 1) + pG/I$, converts the ODE to a tractable form, $z_\xi z_\xi = \mu z^\eta - \sigma z$ where $\mu = V_s^2/(I(p + a))$, $\eta = 1 + p - kp$, and $\sigma = 1/[I(kp + a)]$.

Direct integration then yields:

$$u_\xi \equiv v \equiv z^p = B \cos^{\frac{2}{k-1}}(\beta \xi), \quad (6)$$

with $B = (\mu/[\beta^2 s(s - 1)])^{1/(k-1)}$, $\beta = \sqrt{\sigma}(1 - \eta)/2$, and $s = pI$.

The existence of such a trigonometric solution in the nonlinearly dispersive LWA suggests the possibility of finite-width solutions that essentially consist of a single arch of the profile of Eq. (6), similar to what has been derived for uniform chains [1]. Among the most notable properties of such solutions that are testable both experimentally and numerically are the amplitude-velocity scaling $B \sim V_s^{2/(k-1)}$ (which is similar to the single-species case [1, 2]) and the solution width π/β (which explicitly depends on the mass ratio). We have obtained an analytical expression for the width that is valid for all k , but the formula is too lengthy to write explicitly in the general case. The expression for β in the case of Hertzian interactions (i.e., $k = 3/2$) is $\beta = (30 - 8\omega + 8\omega^2)^{-1}(\sqrt{3}(8 - 5\omega + 5\omega^2 - \sqrt{4 - 4\omega + 13\omega^2 - 18\omega^3 + 9\omega^4})((1 + \omega^2)(15 - 4\omega + 4\omega^2)))/(D^2(34 - 42\omega + 59\omega^2 - 34\omega^3 + 17\omega^4 + (-8 + 5\omega - 5\omega^2)\sqrt{4 - 4\omega + 13\omega^2 - 18\omega^3 + 9\omega^4}))^{1/2}$, where $\omega = m_2/m_1$. This result, which is one of the main findings of the present work, generalizes all previously known limiting cases – namely $m_1 = m_2$, for which $\beta = \sqrt{10}/(5D)$ [resulting in pulses extending to $5\pi/\sqrt{10} \approx 5$ sites], and $m_1 \gg m_2$ [resulting in pulses of $\sqrt{10}\pi \approx 10$ sites (composed of 5 cells with 2 sites each)] [1].

Comparison between experiments, numerical simulations, and theory. To begin, we examine the scaling of the maximum dynamic force F_m of the solitary waves versus their propagation speed V_s . The theory predicts that $F_m \sim B^k \sim V_s^{2k/(k-1)}$, which for $k = 3/2$ yields $V_s \sim F_m^{1/6}$. We tested this experimentally using a 1:1 steel:PTFE dimer chain by dropping the striker (a stainless steel bead) from initial heights ranging from 0 m to 1.2 m. We placed sensors in beads 15 and 34 and measured the corresponding peak force. We averaged their amplitudes [$F_m = (F_{15} + F_{34})/2$] and obtained the corresponding wave speed (V_s) using time-of-flight measurements. We calculated these diagnostics similarly in our numerical simulations. As shown in Fig. 3(a), we obtain very good agreement between numerics and experiments. A least-squares fit of the numerical simulations (using the experimental configuration of 38 beads and removing gravity) yields $V_s \sim F_m^{0.1666}$, in excellent agreement with the theory (despite the small number of particles).

To better highlight some of the interesting dynamics of dimer chains, we examined the evolution of the solitary-wave width (the full width at half maximum, or FWHM) as the wave progresses down the chain of beads. As shown in Fig. 3(b), the numerical and experimental results are in very good agreement with each other and with the ‘‘homogenized’’ theory (which should be expected to capture the average of the relevant os-

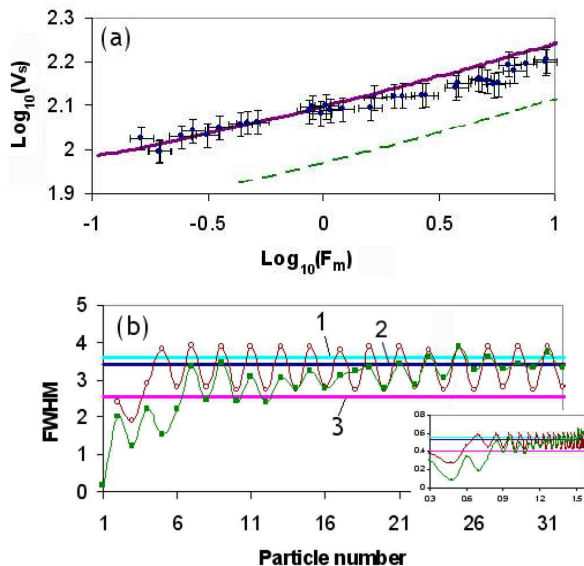


FIG. 3: (Color online) Comparison of experiments, numerical simulations, and theory. (a) Scaling of the maximum dynamic force F_m versus propagation velocity V_s in a 1:1 stainless steel:PTFE chain. The numerical simulations are shown by the solid curve and the experimental results are shown by points (with error bars). The dashed curve shows the numerical results using the elastic modulus $E = 0.6$ GPa for PTFE, the nominal static value reported in most of the literature [13, 33]. (b) Evolution of solitary wave width (full width at half maximum, or FWHM) as a function of bead number (also shown as a log-log plot in the inset). The experimental values are shown by solid (green) squares and the numerical values are shown by open (red) circles. (In both cases, we include curves between the points as visual guides.) The theoretical value for the FWHM with $m_1 \gg m_2$ is given by line (1), that for the 1:1 steel:PTFE chain is given by (2), and that for a homogeneous chain is given by (3).

cillations). The F_m values in the numerics and experiments alternate from one bead to another because consecutive beads are composed of different materials. As one can see from Fig. 3(b), the average FWHM of the dimer is decidedly different from that of a homogeneous chain ($m_1 = m_2$) and even from that of the $m_1 \gg m_2$ limiting case. It is best captured by the theoretical calculation above (for the proper ratio of masses), clearly evincing the relevance of our theoretical approach. As a quantitative measure, the relative error of the theoretical prediction versus the computational-average FWHM is 22.8% for $m_1 = m_2$, 9.2% for $m_1 \gg m_2$, and 2.5% for the relevant mass ratio. In conjunction with the theoretical analysis developed in this paper, our experiments and numerics reveal that the equilibrium conditions (in a horizontal chain) for the wave width are achieved even at very short propagation distances (i.e., with a very small number of beads). For vertical chains of beads that contain a large number of particles (several hundred or more)

or are excited by smaller-amplitude pulses, the presence of the nonuniform gravitational precompression should be taken into account. As discussed in [7], this leads to a 1/3 power law scaling in the wave width as a function of particle number.

Conclusions. We examined the propagation of solitary waves in heterogeneous, periodic chains of granular media using experiments, numerical simulations, and theory. Using different periodicities, we found that such heterogeneous systems robustly support the formation and propagation of highly localized nonlinear solitary waves (with appropriate widths that depend on the periodicity). We used force-velocity scaling (which is the same as for homogeneous chains) and solitary-wave width (which depends on the mass ratio of the dimer materials) as relevant benchmarks for the very good agreement between our three approaches. This qualitative and quantitative understanding of the dimer dynamics also paves the way for studies in increasingly heterogeneous media (e.g., trimers) in both one and higher dimensions, as well as of more complex (optical) modes in such systems.

Acknowledgements We acknowledge support from the Caltech Information Science and Technology initiative (M.A.P.), start-up funds from Caltech (C.D.), and NSF-DMS and CAREER (P.G.K.). I.S. performed his work as a visiting student of GALCIT at Caltech. We thank A. Molinari and V. F. Nesterenko for useful discussions.

* Electronic address: daraio@caltech.edu

-
- [1] V. F. Nesterenko, *Dynamics of Heterogeneous Materials* (Springer-Verlag, New York, NY, 2001).
 - [2] C. Daraio et al., Phys. Rev. E **73**, 026610 (2006).
 - [3] C. Coste et al., Phys. Rev. E **56**, 6104 (1997).
 - [4] E. J. Hinch and S. Saint-Jean, Proc. Royal Soc. London A **455**, 3201 (1999).
 - [5] E. Hascoët and H. J. Herrmann, Eur. Phys. Journal B **14**, 183 (2000).
 - [6] M. Manciu et al., Physica D **157**, 226 (2001).
 - [7] J. Hong and A. Xu, Phys. Rev. E **63**, 061310 (2001).
 - [8] J. Hong and A. Xu, App. Phys. Lett. **81**, 4868 (2002).
 - [9] J. Hong, Phys. Rev. Lett. **94**, 108001 (2005).
 - [10] C. Daraio et al., Phys. Rev. Lett. **96**, 058002 (2006).
 - [11] R. Doney and S. Sen, Phys. Rev. Lett. **97**, 155502 (2006).
 - [12] L. Vergara, Phys. Rev. E **73**, 066623 (2006).
 - [13] C. Daraio et al., Phys. Rev. E **72**, 016603 (2005).
 - [14] V. F. Nesterenko et al., Phys. Rev. Lett. **95**, 158702 (2005).
 - [15] S. Job et al., Phys. Rev. Lett. **94**, 178002 (2005).
 - [16] A. Sokolow et al., Europhys. Lett. **77** (2007).
 - [17] P. Rosenau and J. M. Hyman, Phys. Rev. Lett. **70**, 564 (1993).
 - [18] R. Reigada et al., Chaos **13**, 646 (2003).
 - [19] D. K. Campbell et al., Chaos **15**, 015101 (2005).
 - [20] J. Ford, Phys. Rep. **213**, 271 (1992).
 - [21] Y. S. Kivshar and G. P. Agrawal, *Optical Solitons: From Fibers to Photonic Crystals* (Academic Press, San Diego,

- California, 2003).
- [22] J. Fleischer et al., *Opt. Express* **13**, 1780 (2005).
 - [23] O. Morsch and M. Oberthaler, *Rev. Mod. Phys.* **78**, 179 (2006).
 - [24] M. Peyrard, *Nonlinearity* **17**, R1 (2004).
 - [25] H. Bilz et al., *Phys. Rev. Lett.* **48**, 264 (1982).
 - [26] P. C. Dash and K. Patnaik, *Prog. Theor. Phys.* **65**, 1526 (1981).
 - [27] M. J. Rice and E. J. Mele, *Phys. Rev. Lett.* **49**, 1455 (1982).
 - [28] A. A. Sukhorukov and Y. S. Kivshar, *Opt. Lett.* **27**, 2112 (2002); R. Morandotti et al., *Opt. Lett.* **29**, 2890 (2002).
 - [29] M. Sato et al., *Rev. Mod. Phys.* **78**, 137 (2006).
 - [30] A.-C. Hladky-Hennion and G. Allan, *J. of App. Phys.* **98**, 054909 (2005).
 - [31] *ASM Metals Reference Book* (American Society for Metals, Metals Park, OH, 1983), 2nd ed.
 - [32] <http://www.efunda.com>.
 - [33] www.dupont.com/teflon/chemical/.
 - [34] S. Pnevmatikos et al., *Phys. Rev. B* **33**, 2308 (1986).
 - [35] To investigate optical excitations, it would be necessary to employ a fundamentally different and more complex framework involving a single precompressed bead and excitations of prescribed frequency in the corresponding linear-spectrum gap of such a setting.